Organic Geochemistry 40 (2009) 111–118

Contents lists available at ScienceDirect

Organic Geochemistry

journal homepage: www.elsevier.com/locate/orggeochem

The measurement of D/H ratio in alkenones and their isotopic heterogeneity

Valérie F. Schwab *, Julian P. Sachs

School of Oceanography, University of Washington, Box 355351, Seattle, WA 98195, USA

ARTICLE INFO

Article history:
Received 26 February 2008
Received in revised form 22 August 2008
Accepted 5 September 2008
Available online 14 October 2008

ABSTRACT

Previous paleoenvironmental studies reported the δD values of a mixture of coeluting alkenones. Here, we present a semi-preparative normal-phase high-performance liquid chromatography–mass spectrometry (NP-HPLC–MS) method for purifying long chain (C_{37} and C_{38}) unsaturated methyl and ethyl ketones (alkenones) on the basis of chain length and degree of unsaturation.

The method was applied to purify alkenones in suspended particles and surface sediments from a site in Chesapeake Bay, eastern USA. The hydrogen isotopic composition of di- and triunsaturated C_{37} and C_{38} alkenones differed significantly on the basis of chain length and the degree of unsaturation, demonstrating the importance of gas chromatography–isotope ratio-mass spectrometry (GC–irMS) analysis of individual alkenones for accurate paleoenvironmental reconstruction. Constant fractionation factors between alkenones with different chain length but the same degree of unsaturation ($\alpha_{C_{37:2}-C_{38:2}}$ and $\alpha_{C_{37:3}-C_{38:3}} = 1.01$) and those with the same chain length but different degree of unsaturation ($\alpha_{C_{37:2}-C_{37:3}}$ and $\alpha_{C_{38:2}-C_{38:3}} = 0.97$) in all samples suggest that the values may represent hydrogen isotope fractionation associated with elongation and desaturation during alkenone biosynthesis.

1. Introduction

Long chain C_{37}–C_{39} methyl and ethyl alkenones and related alkenoates are biosynthesized exclusively by certain haptophyte algae, including mainly the cosmopolitan coccolithophorid *Emiliania huxleyi* and the closely related species *Gephyrocapsa oceanica* (Volkman et al., 1980a; Marlowe et al., 1984). They are of interest to paleoceanographers (Sachs et al., 2000) because their degree of unsaturation can be used to reconstruct sea surface temperatures (e.g., Marlowe et al., 1984; Brassell et al., 1986; Prahl and Wakeham, 1987; Prahl et al., 1988; Müller et al., 1998), their carbon isotopic composition can be used to reconstruct atmospheric CO_2 concentrations (Jasper and Hayes, 1990; Pagani et al., 1999; Benthien et al., 2002, 2005) and, most recently, their hydrogen isotopic composition can be used to reconstruct hydrologic (Pahnke et al., 2007; van der Meer, et al., 2007), salinity (Schouten et al., 2006; Sachse and Sachs, 2008) and depositional changes (Englebrecht and Sachs, 2005).

Yet, stable hydrogen isotope analysis of alkenones has been limited in part by a time- and labor-intensive purification regimen that was required before isotopic analyses could be conducted using gas chromatography–isotope ratio-mass-spectrometry (GC–irMS). The purification techniques typically involved multiple wet chemical separations such as hydrolysis, column chromatography with regular and $AgNO_3$-adducted silica gel and urea adduction that were time consuming and often low-yielding (Englebrecht and Sachs, 2005; Pahnke et al., 2007). Moreover, purification was not optimal since the alkenones were not separated individually and the alkenoates that coeluted with the alkenones were typically not quantitatively recovered. Baseline separation between the different unsaturated alkenones of a given chain length cannot be achieved with GC–irMS techniques. Consequently, previous alkenone D/H ratio values were determined by integrating a mixture of coeluting alkenones. Due to significant hydrogen isotope differences between alkenones with different degrees of unsaturation (D'Andrea et al., 2007), this approach may have resulted in the misinterpretation of alkenone δD values.

In this paper, we present a semi-preparative high-performance liquid chromatography–mass spectrometry (HPLC–MS) technique for purifying and separating the alkenones on the basis of carbon chain length and degree of unsaturation. The method was developed to minimize sample handling and maximize recovery so that compound-specific hydrogen isotope analysis could be performed on alkenone-deficient samples. We also report the first individual δD values of di- and triunsaturated C_{37} and C_{38} alkenones and C_{36} alkenoates from suspended particles and surface sediments collected from Chesapeake Bay estuary, eastern USA. Hydrogen isotope compositions of individual alkenones provide insights into their biosynthetic origin.

2. Material and methods

2.1. Study site and sample collection

Sediment and suspended particles were collected from the R/V Kerhin on May 25, 2006 in the mesohaline area of Chesapeake Bay

* Corresponding author. Tel.: +1 206 616 4658.
E-mail address: vfschwab@u.washington.edu (V.F. Schwab).

0146-6380/$ - see front matter © 2008 Elsevier Ltd. All rights reserved.
doi:10.1016/j.orggeochem.2008.09.013

(CB). Located in the Mid-Atlantic region of North America, CB is the largest estuary in the USA (11,500 km^2), with a length of 300 km and a variable width of up to 30 km. Its physical, chemical and biological characteristics have been extensively studied because of the progression of eutrophication and anoxia as a result of anthropogenic activity (e.g., Taft et al., 1980; Officer et al., 1984; Cooper and Brush, 1991; Malone, 1992; Harding and Perry, 1997; Austin, 2004). Sampling was conducted at station CB4.2C (38.6448°N; 76.4177°W) of the Chesapeake Bay Maryland Monitoring Program. Located downstream of a turbidity maximum at the mouth of the Susquehanna River, southwest of Tilghman Island and ca. 220 km upstream from the estuary mouth, the site is characterized by a depth of 26 m, high primary productivity (up to 45.4 μg/l chlorophyll *a* in April and May in 2002 to 2007, and 14.1 μg/l during our visit in May 2006), and bottom-water anoxia during summer (1.5 to 0 mg/l mean bottom water dissolved oxygen from May to September 2006; http://www.cheasapeakebay.net). Additional information on the seasonal and inter-annual variation in primary productivity, pH and oxygen concentration may be obtained from the website of the Chesapeake Bay Monitoring Program (http://www.cheasapeakebay.net).

At the time of sampling, the surface water temperature was 16.8 °C and its salinity 12.8 PSU. High alkenone concentrations in surface waters (<3) of up to 4.6 μg/l were reported at this location by Mercer et al. (2005). *E. huxleyi* and *G. oceanica* are the most common alkenone-producing species in the bay (Marshall, 1980, Chesapeake Bay Program).

Near-surface sediments were collected with a Shipek-type sediment grab sampler. The upper 2 cm, which were green-yellow in color, were skimmed off with a spatula and immediately frozen at −20 °C. Suspended particles were collected by filtration through pre-combusted (450 °C, 4 h) Whatman GF/F filters (293 mm) and immediately frozen at −20 °C. Water was pumped from 1 and 5 m depth with a pneumatic pump (Lutz Pumps, Inc., Norcross, GA) through plastic tubing attached to a conductivity–temperature–depth (CTD) instrument.

2.2. Lipid extraction and pre-treatment

As standards, n-C_{37} alkane and 2-nonadecanone (C_{19} ketone; Sigma–Aldrich) were added to both freeze-dried sediment and filters prior to extraction with an automated solvent extractor (ASE-200, Dionex Corp., Sunnyvale, CA, USA). Each sample was extracted three times for 5 min with a mixture of dichloromethane and methanol, (DCM/MeOH, 9:1 v/v) under N_2 at 150 °C and at 1500 psig. The solvent was removed under a stream of N_2 using a Turbovap system (Caliper, Hopkinton, MA, USA). The extracts were fractionated into four parts using column chromatography (1.3 × 26.5 cm) with ca. 16 g pre-combusted (6 h at 500 °C) Al_2O_3 (80–200 mesh) deactivated with 5 wt% H_2O. The first fraction (F1) was eluted with 50 ml hexane/DCM (9:1, v/v) and contained hydrocarbons, F2 was eluted with 60 ml hexane/DCM (1:1, v/v) and contained aromatics and ketones and F3 was eluted with 40 ml DCM/MeOH (1:1, v/v) and contained alcohols. Polar compounds, including most chlorin and carotenoid pigments, were eluted in F4 with 40 ml of 100% MeOH. The fractions were dried under a stream of N_2. Elemental sulfur was removed from F1 and F2 by passing them through a column (1.3 × ca. 3 cm) of activated Cu powder (40–100 mesh). The copper was activated with three column volumes of 2 N HCl and rinsed successively with three column volumes of each water, MeOH, acetone and DCM.

The alkenones and alkenoates, in F2, were identified using GC-MS with an Agilent (Santa Clara, CA, USA) 6890 N gas chromatograph equipped with an Agilent 5983 autosampler, a split-splitless injector operated in splitless mode, and a HP-5 ms column (30 m × 0.32 mm i.d. × 0.25 μm film thickness, Agilent) interfaced to an Agilent 5975 quadrupole mass selective detector (MSD). After an initial period of 7 min at 70 °C the column was heated to 150 °C at 15 °C/min, then at 6 °C/min to 320 °C (held 28 min). The MSD was operated in the electron ionization mode at 70 eV, with a source temperature of 250 °C, an emission current of 1 mA and with multiple-ion detection in the *range m/z* 50–700 at 2.28 scans/s. Alkenones were identified by mass spectral characteristics and GC retention times by comparison with published data (de Leeuw et al., 1980; Volkman et al., 1980a, 1980b; Marlowe et al., 1984; Rechka and Maxwell, 1988).

Alkenones were quantified using GC with-flame ionization detection (GC-FID). The Agilent 6890 gas chromatograph was equipped with an Agilent 5983 autosampler and a programmable temperature vaporization inlet (PTV) operated in splitless mode. A 60 m Varian Chrompac CP-Sil 5 column (0.32 mm × 0.25 μm) was used with He as carrier gas (1.6 ml/min). The oven temperature program was: 100–275 °C at 40 °C/min, to 315 °C (held 37 min) at 2 °C/min and finally at 5 °C/min to 325 °C (held 5 min). Quantification was performed by comparing integrated peak areas with that of the *n*-C_{36} alkane standard.

2.3. Alkenone separation using semi-preparative HPLC and screening with MS

An Agilent High-Performance Liquid Chromatograph 1100 series equipped with an automatic injector, quaternary pump, integrated fraction collector and Chemstation chromatography software was used. Injection volume was typically 100 μl. A Prevail Cyano column (250 mm × 4.6 mm, 5 μm particle size; Alltech, Deerfield CA) maintained at 30 °C was used. Compound classes were separated using a mixture of hexane and DCM as detailed in Table 1. The elution of compounds of interest was monitored with an Agilent 1100 SL mass spectrometer equipped with a multimode source operated in positive atmospheric pressure chemical ionization (APCI+) mode on ca. 2% of the total flow that was split from the eluent using an adjustable flow splitter (ASI, El Sobrante, CA, USA). A Waters (Milford, MA, USA) 510 pump was used to add a flow of 0.3 ml/min 2,2,4-trimethylpentane to the 2% split in order to supply sufficient solvent to the APCI source for optimal ionization efficiency. Conditions for APCI-MS were: gas temperature 350 °C, vaporizer temperature 250 °C, drying gas (N_2) flow 12 l/min, nebulizer pressure 35 psig, capillary voltage 2.5 kV, corona current 6 μA and corona charge voltage 2 kV. Mass spectra were obtained in full scan mode (*m/z* 200–800) with the following settings: fragmentor 140, gain 1.0, threshold 150 and step size 0.1.

The solvent (100 μl) used to dissolve the alkenone fraction was 10% DCM in hexane. To ensure good separation and peak shape, <40 μg of an individual alkenone was injected on the HPLC instrument. The elution times of individual alkenones had been determined previously from multiple injections. Alkenone concentration changes between samples resulted in retention time variation of ca. ±10 s. Therefore, to ensure complete collection and a good separation of the target compounds, HPLC fractions were collected during multiple adjacent 30 s intervals before and after

Table 1
HPLC solvent gradient[a]

Time (min)	A (%)	B (%)	C (%)	Flow rate (ml/min)
0	0	50	50	1
35	0	50	50	1
36	55	45	0	1
41	55	45	0	1.5
42	0	50	50	2
54	0	50	50	2

[a] A, dichloromethane; B, hexane; C, 4% dichloromethane in hexane.

the expected elution time of each compound. The accuracy of separation was evaluated using HPLC-MS with the extracted ions *m/z* 545 and 543 for the di- and triunsaturated C_{38} alkenones, respectively, and 531 and 529 for the di- and triunsaturated C_{37} alkenones, respectively. The alkenoates were obtained by combining the different fractions according to the mass spectra with the extracted ions *m/z* 545, 547, 559 and 561. To ensure complete recovery, if an analyte was split between two or more fractions they were recombined. The collected fractions were covered with a sheet of Al foil and placed in a fume hood to allow the solvent to evaporate overnight. Each sample was analyzed using GC-FID before and after the HPLC–MS treatment in order to determine the recovery and purity of each alkenone.

2.4. Hydrogen isotope analysis

The amount of alkenones required for adequate intensities on the GC-irMS system (2000 mV) was 300 ng. Their D/H ratio was determined using GC/TC/irmMS with a DELTA V PLUS irMS system (Thermo Scientific, Waltham, MA, USA). The gas chromatograph (Trace Ultra, Thermo) was equipped with a split–splitless injector operated in splitless mode at 300 °C, a TRIPLUS autosampler (Thermo Scientific, Waltham, MA, USA) and a DB5 ms column (60 m × 0.32 mm × 0.25 μm, Agilent) programmed from 80 to 200 °C at 20 °C/min, then at 4 °C/min to 320 °C (held 30 min). He was used as carrier gas at a constant flow of 1 ml/min. Compounds were pyrolyzed in an empty ceramic tube heated to 1420 °C, that was pre-activated by injecting 1μl of *n*-hexane. Samples of 1 μl were co-injected with 1 μl of a standard comprising C_{38} and C_{41} *n*-alkanes with known hydrogen isotopic composition bracketing the compound of interest. Isotopic values were calculated with ISODAT software pack 2 (Thermo-Fisher, Bremen, Germany) using the two co-injected standards.

Instrument performance and the H_3^+ factor were determined on a daily basis using a tank of H_2 reference gas and a mixture of *n*-alkanes (C_{14} to C_{44}) of known isotopic composition. Hydrogen isotopic composition of *n*-C_{14} to *n*-C_{36} *n*-alkane was determined off line using a thermo chemical elemental analyzer (TC/EA; Thermo-Fisher, Bremen, Germany) interfaced to the DELTA V PLUS irMS system via a Conflo III combustion interface (Thermo-Fisher, Bremen, Germany). The *n*-C_{38}, *n*-C_{41} and *n*-C_{44} standards used for δD corrections and added to the *n*-alkane mixture for the H_3^+ factor calculation were acquired from A. Schimmelmann (Indiana University, Bloomington, Indiana). The average isotopic difference between the GC-irMS-measured and off line-determined values was 3.9‰ (n = 3630, 165 runs with 22 peaks). The H_3^+ factor was lower than 4 and stable during the measurements.

We observed that even with a very clean baseline the standardized background integration method could sometimes change the hydrogen isotopic composition of the target compounds by up to 15‰ due to the co-elution of small siloxane peaks. In these cases the results are not discussed. The hydrogen isotope composition and standard deviation of each compound were determined by individual background integration. We report δD values averaged from at least three separate analyses of the sample. The precision of our alkenone δD measurements, as determined by the standard deviation of the three or more measurements, was 4.2‰

3. Results and discussion

3.1. Alkenone distribution

The distribution of alkenones was similar in suspended particle and surface sediment samples, with a predominance of methyl C_{37} over ethyl C_{38} compounds, an absence of methyl C_{38} alkenones and a higher relative concentration of tri- over di- and tetra-unsaturated alkenones (Fig. 1). Methyl and ethyl C_{36} alkenoates were observed in all samples, with a predominance of di- over triunsaturated analogs.

The concentration of total C_{37}–C_{38} alkenones was 24 μg/g of dry suspended particles at 1 m water depth, 28 μg/g of dry suspended particles at 5 m water depth and 39 μg/g dry sediment. The concentration of the $C_{37:4}$ alkenone was <0.01 μg/g of dry sediment. We do not report the concentration of the $C_{38:4}$ alkenone because our GC conditions resulted in its co-elution with alkenoates and we were unable to quantify it accurately.

3.2. Separation of individual alkenones with HPLC–MS

The cyano column, consisting of silica modified with cyanopropyl groups, represents an intermediate polarity between a silica and a C_{18} column (Marchand et al., 2005). This type of column has been used in geochemical and petroleum research for group-type fractionation (Borgund et al., 2007). Dipole–dipole interactions are believed to aid the retention of polar aliphatic solutes owing to the large dipole moment of the cyano group (Croes et al., 2005). Solute retention on the cyano stationary phase may also be augmented by π–π interactions, as observed with polycyclic aromatic hydrocarbons (PAHs; Horak et al., 2004).

Individual alkenones and alkenoates were well-separated using a normal phase (NP) HPLC method consisting of a cyano column and an isocratic mobile phase of 2% DCM in hexane (Fig. 2). The low molecular weight (MW) aromatic hydrocarbons, short chain ketones and fatty acid esters eluted first, followed by the alkenoates, the C_{38}-alkenones and the C_{37}-alkenones. Alkenone retention times increased with decreasing MW and increasing degree of unsaturation.

As expected for NP chromatography on a cyano column, an increase in the retention time of less hydrophobic solutes was achieved by decreasing the polarity of the mobile phase. Thus, an isocratic program of 100% hexane increased the retention time and resulted in baseline separation of $C_{37:4}$ and $C_{37:3}$, permitting complete collection of both alkenones, with $C_{37:4}$ eluting after $C_{37:3}$. Unfortunately, because of the low concentration of the $C_{38:4}$ alkenone, the separation between $C_{38:4}$ and $C_{38:3}$ was not tested. Nevertheless, the use of 100% hexane required a substantially longer re-equilibration time of the column after each run when the column was cleaned with 55% DCM in hexane. Thus, given the low concentration of tetra-unsaturated C_{37} and C_{38} alke-

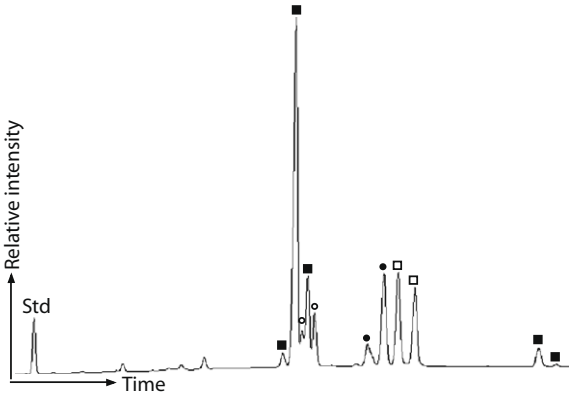

Fig. 1. Partial gas chromatogram showing representative alkenone distributions in surface sediments of Chesapeake Bay. Black squares indicate tetra-, tri- and di-unsaturated methyl C_{37} alkenones, and tri- and di-unsaturated methyl C_{39} alkenones. White squares indicate tri- and di-unsaturated ethyl C_{38} alkenones. Black and white circles indicate methyl and ethyl tri- and di-unsaturated C_{36} alkenoates, respectively.

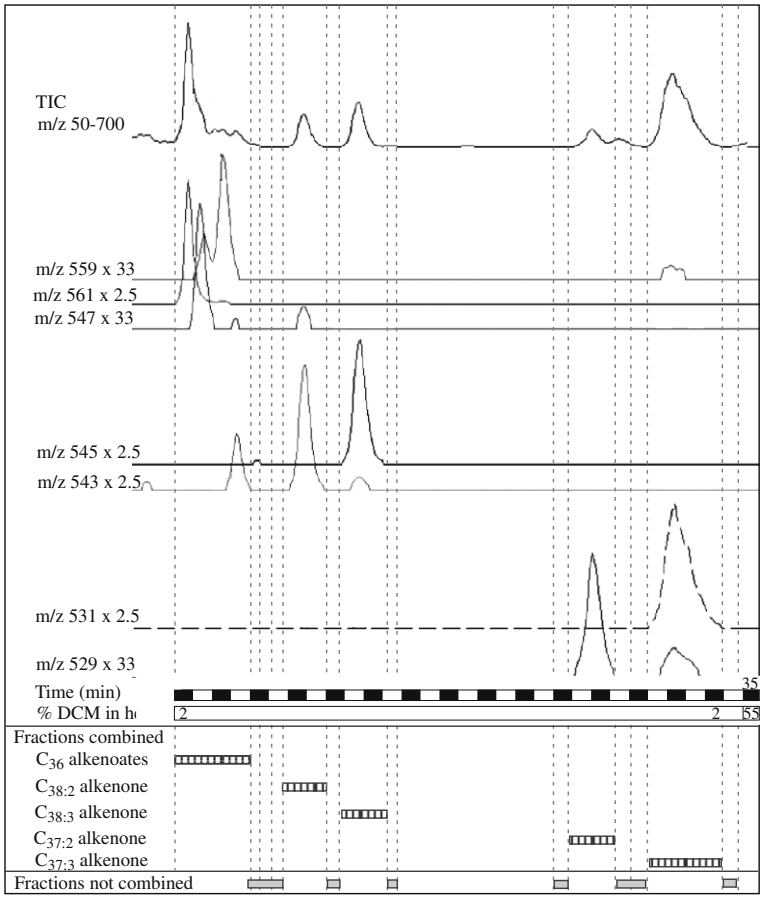

Fig. 2. Partial total ion chromatogram (TIC, *m/z* 50–700) and mass chromatograms of representative HPLC runs. The *m/z* number represents the atomic mass of the ion generated by protonation of individual alkenones and alkenoates. The vertical scales, which were multiplied by the factor to the right of the *m/z* value, indicate the relative intensities of the ion signals. Time in min and the solvent mixture are indicated by black and white bars below the bottom mass chromatogram. The line-filled rectangles at the bottom of indicate the time interval over which HPLC fractions were combined for subsequent δD analyses of: (1) C_{36} alkenoates, (2) $C_{38:2}$ alkenones, (3) $C_{38:3}$ alkenones, (4) $C_{37:2}$ alkenones, and (5) $C_{37:3}$ alkenones. Gray rectangles at the bottom indicate time interval over which fractions were collected and subsequently analyzed using GC-FID in order to quantify the alkenones that were not collected, thus verifying that at least 92% of each alkenone was recovered prior to hydrogen isotopic analysis.

nones in our samples, we opted to use a 2% DCM in hexane mobile phase for the alkenone separations.

The purity of alkenones separated with this HPLC method was evaluated using GC-FID and GC-MSD, revealing very clean fractions (Fig. 3). Comparing the concentration of $C_{37:2}$ and $C_{37:3}$ prior to HPLC purification (i.e. in the F2 fraction) to the concentration of $C_{37:2}$ and $C_{37:3}$ after HPLC, we calculated an HPLC recovery of 98.5% (std. dev. 0.9, $n = 15$). This high recovery, as discussed below, is essential for maintaining the hydrogen isotopic integrity of the sample, while also allowing for D/H analysis of relatively small samples. The method also minimizes sample pre-treatment time since HPLC injection and collection can be automated.

3.3. Hydrogen isotopic effects during normal phase HPLC

Normal- and reversed-phase (RP-) HPLC can cause substantial hydrogen (Turowski et al., 2003; Smittenberg and Sachs, 2007), carbon (Caimi and Brenna, 1997) and nitrogen (Bidigare et al., 1991) isotope fractionation across a chromatographic peak. Quantitative peak collection is therefore essential to maintain isotopic integrity of analytes (Bidigare et al., 1991; Smittenberg and Sachs, 2007). Furthermore, the polarity of the stationary phase has been shown to influence the nature of the isotope fractionation. In NP-HPLC, D-depleted compounds elute more rapidly (Smittenberg and Sachs, 2007), while in RP-HPLC, D-enriched compounds elute first (Caimi and Brenna, 1997; Bidigare et al., 1991; Turowski et al., 2003).

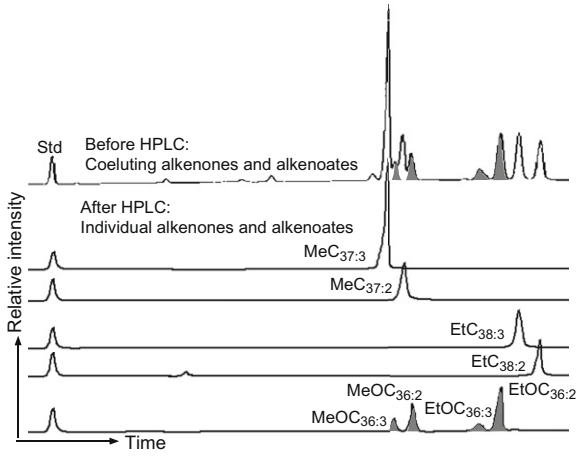

Fig. 3. Partial GC-FID chromatograms from Chesapeake Bay sediment showing F2 fraction prior to HPLC (upper chromatogram) and fractions containing the purified alkenones and alkenoates after semi-preparative HPLC (lower five chromatograms). Alkenoates are indicated by gray shading.

This chromatographic isotope effect (IE) is attributable to the vibrational state of the atoms, which is a function of the mass of the nuclei. The smaller vibration amplitude of deuterium relative to protium, resulting from its greater mass, causes slightly lower average volume and polarizability. Consequently, intermolecular

bonds between D-enriched compounds and non-polar moieties are relatively weaker than intermolecular bonds involving D-depleted compounds and non-polar moieties. In RP-HPLC, characterized by a non-polar stationary phase and a polar mobile phase, D-enriched molecules elute prior to D-depleted molecules, while in NP-HPLC, characterized by a polar stationary phase and a non-polar mobile phase, D-enriched compounds have a stronger retention by the stationary phase and therefore elute later (Turowski et al., 2003; Smittenberg and Sachs, 2007).

Nevertheless, the chromatographic retention mechanisms involving the sum of all physical and chemical interaction processes among solute, stationary and mobile phases remain incompletely understood. Under similar chromatographic conditions, it has been argued that the magnitude of the IEs is a function of the concentration and the molecular structure of the solute that may in turn alter the intermolecular interactions between the stationary phase, the mobile phase and the solute (Turowski et al., 2003). On a cyano column, solute retention primarily involves dipole-dipole interactions for polar aliphatic compounds and π–π interactions for PAHs (Horak et al., 2004; Croes et al., 2005). The cyano groups may interact more strongly with PAHs than with other aromatic hydrocarbons due to the higher number of π-electrons available for π–π interactions (Horak et al., 2004). The strength of the interaction between the solute and the stationary phase may be directly related to the extent of the IEs (Turowski et al., 2003). As with HPLC, GC separations cause an inverse isotope effect. When a non-polar GC column is used, the heavier isotopomers with lower molar volumes elute earlier since the Van der Waals dispersion forces play a dominant role in the solute–stationary phase interaction (Matucha et al., 1991).

To test the effect on the IEs of different molecular structures and concentrations of solute we measured the change in the hydrogen isotope composition across the HPLC peaks of 2-eicosanone (C_{20} ketone) and benz(e)acephenanthrylene (a PAH) standards (Sigma–Aldrich), as well as a $C_{37:3}$ alkenone from the F2 fraction of CB sediment injected at different concentrations. The C_{20} ketone and the $C_{37:3}$ alkenones were evaluated with the same chromatographic conditions used to purify the CB alkenones because they have similar polarities and retention times. However, the higher polarity of the PAH required an increase in the polarity of the mobile phase to 10% DCM in hexane. The resulting chromatograms showed minor distortion of peak symmetry, which may indicate binding site saturation in the stationary phase.

The δD value of each HPLC peak fraction, the % eluted mass and the δD offset are listed in Table 2. The δD reference values of the PAH and C_{20} ketone were obtained by measuring the untreated standard with GC–irMS. The δD reference value of the $C_{37:3}$ alkenone was obtained after purification using HPLC followed by GC–irMS. The procedure was repeated three times with each sample. The standard deviation of three replicates was <4.2‰. The weighted average of the collected fractions gave, within measurement error, the same isotopic values as the reference values (Table 2).

Plotting the offset from the δD value of the pure compound for each chromatographic peak interval against its position within the eluting peak (as the % eluted mass at the time of the fraction col-

Table 2
δD values of fractions collected across HPLC peaks of 2-eicosanone (C_{20}-ketone) and benz(e)phenanthrylene (PAH).[a]

Compound	Fraction	δD (‰)	Std. dev.	Amount of sample eluted (μg)	Mass eluted (%)	δD offset (‰)
C_{20}-ketone	1st	−215.0	2.4	2.7	8.2	−48.1
	2nd	−184.9	3.4	19.0	57.9	−11.6
	3rd	−164.5	3.2	10.6	32.4	49.5
	4th	−115.8	4.3	0.5	1.5	72.1
	weighted avg.	−179.7				
	No HPLC	−175.3	4.5			
	Amount injected			32.0		
PAH	1st	−88.8	3.4	3.0	4.5	−104.6
	2nd	−42.3	5.9	6.8	10.1	−58.8
	3rd	0.4	2.2	12.1	18.6	−16.9
	4th	3.9	5.1	13.4	19.8	−13.4
	5th	9.1	2.7	17.4	25.7	−8.3
	6th	135.5	8.7	14.3	21.2	115.9
	weighted avg.	23.6				
	No HPLC	17.6	7.5			
	Amount injected			67.0		
$MeC_{37:3}$	1st	−259.1	4.2	0.3	1.7	−65.1
	2nd	−207.7	4.8	5.3	39.1	−0.2
	3rd	−209.1	2.3	5.4	39.5	−2.0
	4th	−196.2	2.0	1.6	12.1	14.3
	5th	−166.3	2.7	1.1	7.6	52.0
	Weighted avg.	−204.6				
	No HPLC	−207.5	3.4			
	Amount injected			13.7		
$MeC_{37:3}$	1st	−226.1	0.9	4.0	10.3	−23.4
	2nd	−213.5	4.5	3.9	10.1	−7.6
	3rd	−211.7	2.7	4.2	10.9	−5.3
	4th	−211.5	0.8	3.5	8.9	−5.1
	5th	−210.1	3.1	3.4	8.9	−3.3
	6th	−212.6	1.5	6.9	17.7	−6.5
	7th	−211.5	3.8	6.4	16.5	−5.1
	8th	−187.6	2.1	4.8	12.2	25.5
	9th	−165.0	4.2	1.7	4.3	53.6
	Weighted avg.	−208.3				
	No HPLC	−207.5	3.4			
	Amount injected			38.8		

[a] Eluted mass (%), percentage of the total mass of the compound eluted at the time when the fraction was collected; C_{20}-ketone, 2-eicosanone; PAH, benz(e)acephenanthrylene; $MeC_{37:3}$, triunsaturated C_{37} methyl alkenone; weighted avg., weighted average δD value of the collected fractions noted above; NO HPLC, δD reference value of the compounds directly measured on the GC-irMS.

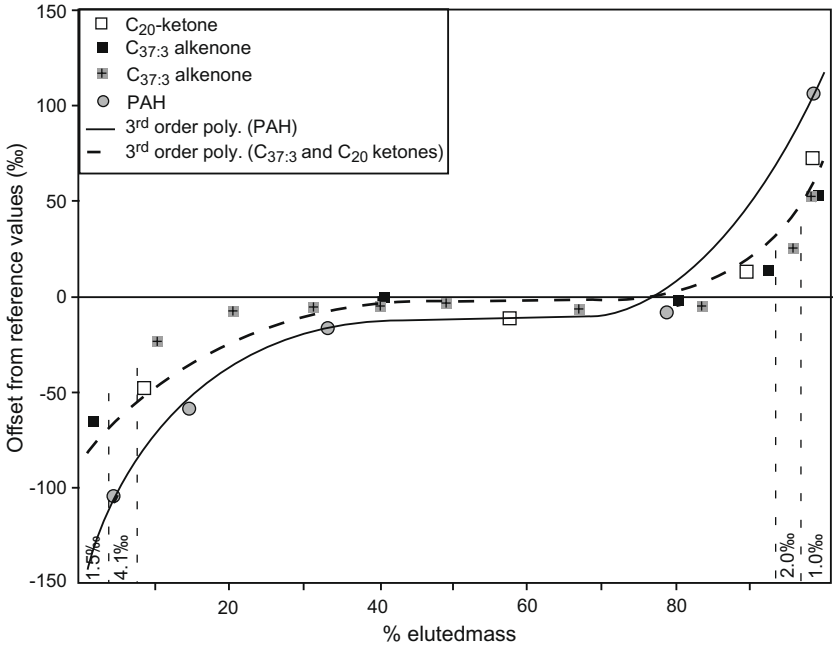

Fig. 4. Hydrogen isotopic variation across an HPLC peak of the $C_{37:3}$ alkenone and two standards, benz(e)acephenanthrylene (PAH) and 2-eicosanone (C_{20} ketone). The *x*-axis is the wt% of the total mass eluted at the time of the fraction collection. The *y*-axis is the offset from the δD value of the pure compound (determined independently from GC-irMS) for the collected fraction. Numbers above the *x*-axis indicate the error in the alkenone δD value that would result if 4% or 8% of the front or back of the peak was not collected. The calculations were based on the 3rd-order polynomial fit to the $C_{37:3}$ alkenone and C_{20}-ketone data (dashed curve). Solid curve shows 3rd order polynomial fit to the PAH data and indicates that the fractionation across an HPLC peak of a PAH differs from that across a non-aromatic, acyclic molecule (see text). Amounts injected are shown in Table 2.

lection) indicates that all three compounds display a similar pattern of isotopic fractionation across the peak, with D-enriched molecules retained relative to D-depleted molecules (Fig. 4). A longer retention time for D-enriched compounds is consistent with their stronger affinity for the stationary phase. Benz(e)acephenanthrylene is characterized by stronger IE relative to both the C_{20} ketone and $C_{37:3}$ alkenone (Fig. 4). Higher IE for the PAH relative to the polar aliphatic solutes is consistent with stronger π–NP than dipole–NP solute interactions. No significant difference in was observed between the C_{20} ketone and $C_{37:3}$ alkenone. According to these results, we conclude that, for chemically and structurally related compounds such as the alkenones and the C_{20} ketone, changes in MW and degree of unsaturation should not significantly affect the IE, even though they significantly affect retention time. Therefore, the IE for each alkenone is likely to remain similar to those observed for the $C_{37:3}$ alkenone and the C_{20} ketone.

We evaluated the effect on alkenone δD values of excluding the extremeties of a chromatographic peak by fitting a third order polynomial equation to δD offsets across the HPLC peak of the $C_{37:3}$ alkenone and the C_{20} ketone (Fig. 4). Omitting 4% (wt) of the front or the back of a peak would cause an error in the hydrogen isotope ratio of ca. 1.5‰ and −1.0‰, respectively, which is within the analytical error of the δD analysis. Omitting 8% of the peak front or 10% of the peak tail would cause an error of 4‰ and −4‰, respectively. These calculations indicate that at least 92% of the HPLC peak should be collected to ensure the accuracy of hydrogen isotope analysis.

3.4. δD values of individual alkenones purified with HPLC

The hydrogen isotope composition of di- and tri-unsaturated C_{37} and C_{38} alkenones, and ethyl and methyl $C_{36:2}$ alkenoates from Chesapeake Bay that were purified with HPLC–MS are listed in Table 3. The δD values of the individual alkenones from suspended particles and sediments were similar within the analytical error but varied widely as a function of chain length and number of double bonds. The C_{38} alkenones were consistently depleted in deuterium by ca.13‰ relative to the C_{37} alkenones. Furthermore, the diunsaturated alkenones were consistently enriched in deuterium relative to the tri-unsaturated alkenones by ca. 23‰. The $C_{36:2}$ methyl and ethyl alkenoates had similar δD values to the $C_{38:2}$ and $C_{38:3}$ alkenones, respectively.

The proposed biosynthetic pathway of the C_{37}–C_{40} alkenones starts from acetyl-SCoA and involves 16 elongation steps by malonyl-SCoA to produce a tetratriacontanoyl-ACP (C_{34}) intermediate (Rontani et al., 2006). The synthesis of C_{37} methyl and C_{38} ethyl alkenones involves the successive chain elongations of tetratriacontanoyl-ACP with malonyl-SCoA and methylmalonyl-SCoA, and subsequent decarboxylations (Rontani et al., 2006). In this scheme the synthesis of methyl and ethyl C_{36} alkenoates involves the elongation pathway of tetratriacontanoyl-ACP with malonate units and a subsequent esterification. Based on the unusual double bond spacing (five CH_2 groups instead of the more common one; de Leeuw et al., 1980) and configuration (E instead of the more common Z; (Rechka and Maxwell, 1988), Rontani et al. (2006) suggested that alkenone $\Delta^{14,21}$ desaturation takes place after the biosynthesis of the carbon skeleton, with progressive desaturation of the diunsaturated alkenones leading to the successive formation of the tri- and tetra-unsaturated analogs. To explain the specificity of the alkenone double bond position, Rontani et al. (2006) hypothesized that the enzyme attached to the carbonyl carbon of the alkenone with the carbonyl-binding site (hydrogen removal) fixed at a constant position.

Similar hydrogen isotopic compositions of individual alkenones strongly indicate that they originate from a common straight chain precursor. Constant fractionation factors between alkenones with different chain length but the same degree of unsaturation ($\alpha_{C_{37:2}-C_{38:2}}$ and $\alpha_{C_{37:3}-C_{38:3}} = 1.01$), and those with the same chain length but different degree of unsaturation ($\alpha_{C_{37:2}-C_{37:3}}$ and $\alpha_{C_{38:2}-C_{38:3}} = 0.97$) in all samples suggest that these values may represent hydrogen isotope fractionation associated with subsequent elongation and desaturation. In cultured *E. huxleyi* and in Greenland lake sediments, D'Andrea et al. (2007) also

Table 3
δD values of individual alkenones purified using HPLC-MS[a]

Sample	Compound	δD (‰)	Std. dev.	$\alpha(C_{37:3}–C_{37:2})$	$\alpha(C_{38:3}–C_{38:2})$	$\alpha(C_{37:3}–C_{38:3})$	$\alpha(C_{37:2}–C_{38:2})$
F-CB4.2	$MeC_{37:3}$	−198.4	1.8	0.97		1.01	
1 m	$MeC_{37:2}$	−175.7	4.3				1.02
	$EtC_{38:3}$	−206.3	2.8		0.98		
	$EtC_{38:2}$	−192.6	1.7				
	$MeOC_{36:2}$	−180.0	2.9				
	$EtOC_{36:2}$	−206.3	3.2				
F-CB4.2	$MeC_{37:3}$	−200.6	5.4	0.97		1.01	
2–5 m	$MeC_{37:2}$	−178.8	2.1				1.02
	$EtC_{38:3}$	−207.6	1.3		0.98		
	$EtC_{38:2}$	−194.8	3.2				
	$MeOC_{36:2}$	−182.7	3.2				
	$EtOC_{36:2}$	−209.3	1.6				
S-CB4.2	$MeC_{37:3}$	−204.6	1.4	0.98		1.02	
0–10 cm	$MeC_{37:2}$	−185.2	4.5				1.01
	$EtC_{38:3}$	−217.0	2.9		0.97		
	$EtC_{38:2}$	−194.0	3.3				

[a] $\alpha(C_X–C_Y) = (C_X + 1000)/(C_Y + 1000)$; F-, suspended particulate sample; S-, sediment sample; $MeC_{37:3}$, triunsaturated C_{37} methyl alkenone; $MeC_{37:3}$ diunsaturated C_{37} methyl alkenone; $EtC_{38:3}$, triunsaturated C_{38} ethyl alkenone; $EtC_{38:2}$, diunsaturated C_{38} ethyl alkenone; $MeOC_{36:2}$, diunsaturated C_{36} methyl alkenoate; $EtOC_{36:2}$, diunsaturated C_{36} ethyl alkenoate.

observed constant hydrogen isotope fractionation between $C_{37:2}$, $C_{37:3}$ and $C_{37:4}$ alkenones, but observed a slightly lower fractionation factor ($\alpha_{C_{37:2}–C_{37:3}}$ and $\alpha_{C_{37:3}–C_{37:4}}$) of 0.94. Englebrecht and Sachs (2005) observed a fractionation factor of ca. 1.01 between the pooled C_{37} and C_{38} alkenones in cultured *E. huxleyi*.

It has been shown that hydrogen isotopic variation occurs at specific positions within *n*-alkyl carbon skeletons (Guiet et al., 2003) and that hydrogen removed during dehydrogenation reactions is D depleted owing to a large kinetic isotope effect associated with the desaturaze enzyme (Chikaraishi et al., 2004, 2005). Indeed, D enrichment of the residual material and D-depletion of the product has been reported for fatty acid desaturation (Zhang and Sachs, 2007). The D depletion of the tri- relative to the di-unsaturated alkenone requires that the two hydrogen atoms removed during desaturation of $C_{37:2}$ to $C_{37:3}$ are depleted in deuterium relative to the hydrogens in the residual $C_{37:2}$. Significant D enrichment of di-unsaturated alkenones might therefore result when they are in low relative abundance to their (desaturated) tri-unsaturated counterparts.

3.5. Implications for paleoclimate studies

Most hydrogen isotope studies of alkenones report a pooled isotopic value for all compounds of a given chain length (i.e., $C_{37:2}$, $C_{37:3}$ and $C_{37:4}$) measured together (Englebrecht and Sachs; 2005; Pahnke et al., 2007; van der Meer et al., 2007). Significant differences in the δD values of alkenones with differing numbers of unsaturation imply that combining alkenones that have the same chain length but differing numbers of double bonds could introduce substantial inaccuracies in estimates of environmental D/H signatures. Changes in the relative abundance of di- and tri-unsaturated C_{37} alkenones resulting from sea surface temperature changes would cause, for example, changes in the δD value of the combined C_{37} alkenones even if no change in the δD value of the individual $C_{37:2}$ and $C_{37:3}$ alkenones occurred. In such cases where alkenones with different degrees of unsaturation are combined prior to D/H analysis it is suggested that a lack of co-variation between the unsaturation ratio (i.e., $U^{k'}_{37} = C_{37:2}/(C_{37:3} + C_{37:2})$) (Prahl and Wakeham, 1987) and the δD values may be used as a criterion to evaluate the extent to which changes in the relative abundance of the di- and tri-unsaturated alkenones may have caused changes in the combined ($C_{37:3} + C_{37:2}$) alkenone δD values. If the $U^{k'}_{37}$ and the $\delta D_{C37:3+C37:2}$ values do not co-vary, then it is likely that changes in the relative proportion of the two alkenones were not an important cause of changes in $\delta D_{C37:3+C37:2}$ values.

Applying this criterion to the downcore alkenone δD records from the Panama Basin in Pahnke et al. (2007) and the Mediterranean Sea in van der Meer et al. (2007), we conclude that changes in the relative abundance of the C_{37} alkenones were not likely to have been substantially influenced by changes in the relative abundance of $C_{37:3} + C_{37:2}$. In the case of the downcore record from the Bermuda Rise in Englebrecht and Sachs (2005) it is possible that changes in the unsaturation ratio substantially influenced the downcore changes in the C_{37} alkenone δD values, but the number of data points is too few for a conclusive evaluation.

Furthermore, it has been argued that the extent of D/H fractionation in lipids with varying numbers of double bonds may be directly related to the relative production flux of each unsaturated analog (Chikaraishi et al., 2004). Consequently, differing apparent D/H fractionation factors for di-and tri-unsaturated alkenones may be caused by temperature-induced changes in the production of di-, tri- and tetra-unsaturated alkenones. In that case, we would expect alkenone δD values to be sensitive to temperature, a prediction not borne out by the coccolithophorid culture study by Schouten et al. (2006), but in need of further evaluation. As above, we suggest that a co-variation between alkenone-derived surface water temperatures and alkenone δD values might be cause for concern; a lack of co-variation would be more likely to lead to robust paleoenvironmental conclusions.

4. Conclusions

A method for purifying individual alkenones for hydrogen isotopic analysis using NP-HPLC–MS was presented, using a cyano column and a mobile phase consisting of 2% DCM in hexane eluted isocratically. The method minimizes sample handling and maximizes analyte recovery so that compound-specific hydrogen isotope analyses can be performed on alkenone-deficient samples. Measurements of δD values across individual HPLC peaks of standards and the $C_{37:3}$ alkenone from Chesapeake Bay sediments demonstrate the necessity of collecting at least 92% of the peak in order to maintain isotopic integrity of individual alkenones and compounds with similar structure.

This method was used to isolate di- and tri-unsaturated C_{37} and C_{38} alkenones and C_{36} alkenoates, from suspended particles and surface sediments from station CB 4.2C in the Maryland section of Chesapeake Bay, eastern USA. δD values varied by 13‰ for di- relative to tri-unsaturated alkenones, and 23‰ for C_{37} relative to C_{38} alkenones. Such hydrogen isotope differences between individual alkenones implies that δD values obtained by measuring a

suite of alkenones with a single chain length but different numbers of unsaturations, a method used in previous studies that was unable to measure individual alkenone δD values, could result in downcore alkenone δD variations that were caused by temperature related changes in the unsaturation ratio rather than by changes in water δD values or D/H fractionation during lipid synthesis resulting from other environmental parameters. To avoid this possibility it is necessary to measure δD values on individual alkenones.

Constant fractionation factors between alkenones with different chain length but the same degree of unsaturation ($\alpha_{C_{37:2}-C_{38:2}}$ and $\alpha_{C_{37:3}-C_{38:3}}=1.01$), and those with the same chain length but different degrees of unsaturation ($\alpha_{C_{37:2}-C_{37:3}}$ and $\alpha_{C_{38:2}-C_{38:3}}=0.97$) in all samples suggest that these values may represent hydrogen isotope fractionation associated with elongation and desaturation during alkenone biosynthesis.

Acknowledgements

Funding was provided to J.P. Sachs by The American Chemical Society through Petroleum Research Fund Grant 46937-AC2, by the US National Science Foundation through Grants 0639640 and 0624954, and by the Gary Comer Science and Education Foundation. The Swiss National Science Foundation is thanked for the postdoctoral fellowship awarded to V.F. Schwab. We thank R. Smittenberg, O. Kawka and D. Sachse for assistance in the laboratory. We are grateful to R. Smittenberg, K. Pahnke and J.V. Lavrič for their insights and fruitful discussions. And we thank R. Younger, captain of the R/V Kerhin, from which the Chesapeake Bay samples were collected. Y. Huang and an anonymous reviewer are gratefully acknowledged for their comments.

Associate Editor—**S. Schouten**

References

Austin, J.A., 2004. Estimating effective longitudinal dispersion in the Chesapeake Bay. Estuarine Coastal and Shelf Science 60, 359–368.

Benthien, A., Andersen, N., Schulte, S., Müller, P.J., Schneider, R.R., Wefer, G., 2005. The carbon isotopic record of the $C_{37:2}$ alkenone in the South Atlantic: Last Glacial Maximum (LGM) vs. Holocene. PALAEO 221, 123–140.

Benthien, A., Andersen, N., Schulte, S., Müller, P.J., Schneider, R.R., Wefer, G., 2002. Carbon isotopic composition of the $C_{37:2}$ alkenone in core–top sediments of the South Atlantic Ocean: effects of CO_2 and nutrient concentrations. Global Biogeochemical Cycles 16. doi:19.102/2001GB001433.

Bidigare, R.R., Kennicutt, M.C., Keeney-Kennicutt, W.L., Macko, S.A., 1991. Isolation and purification of chlorophylls a and b for the determination of stable carbon and nitrogen isotope compositions. Analytical Chemistry 64, 130–133.

Borgund, A.E., Erstad, K., Barth, T., 2007. Normal phase high performance liquid chromatography for fractionation of organic acid mixtures extracted from crude oils. Journal of Chromatography A 1149, 189–196.

Brassell, S.C., Eglinton, G., Marlowe, I.T., Pflaumann, U., Sarntheim, M., 1986. Molecular stratigraphy: a new tool for climatic assessment. Nature 320, 129–133.

Caimi, R.J., Brenna, J.T., 1997. Quantitative evaluation of carbon isotopic fractionation during reversed-phase high-performance liquid chromatography. Journal of Chromatography A 757, 307–310.

Chikaraishi, Y., Suzuki, Y., Naraoka, H., 2004. Hydrogen isotopic fractionations during desaturation and elongation associated with polyunsaturated fatty acid biosynthesis in marine macroalgae. Phytochemistry 65, 2293–2300.

Chikaraishi, Y., Matsumoto, K., Ogawa, N.O., Suga, H., Kitazato, H., Ohkouchi, N., 2005. Hydrogen, carbon and nitrogen isotopic fractionations during chlorophyll biosynthesis in C_3 higher plants. Phytochemistry 66, 911–920.

D'Andrea, W.J., Liu, Z., Da Rosa, A.M., Wattley, S., Herbert, T.D., Huang, Y., 2007. An efficient method for isolating individual long-chain alkenones for compounds-specific hydrogen isotope analyses. Analytical Chemistry 79, 3430–3435.

Cooper, S.R., Brush, G.S., 1991. Long-term history of Chesapeake Bay anoxia. Science 254, 992–996.

Croes, K., Steffens, A., Marchand, D.H., Snyder, L.R., 2005. Relevance of π–π and dipole–dipole interactions for retention on cyano and phenyl columns in reversed-phase liquid chromatography. Journal of Chromatography A 1098, 123–130.

Englebrecht, A.C., Sachs, J.P., 2005. Determination of sediment provenance at drift sites using hydrogen isotopes and unsaturation ratios in alkenones. Geochimica et Cosmochimica Acta 69, 4253–4265.

Guiet, S., Robins, R.J., Lees, M., Billault, I., 2003. Quantitative ^{2}H NMR analysis of deuterium distribution in petroselinic acid isolated from parsley seed. Phytochemistry 64, 223–227.

Harding Jr., L.W., Perry, E.S., 1997. Long-term increase in phytoplankton biomass in Chesapeake Bay, 1950–1994. Marine Ecology Progress Series 157, 39–52.

Horak, J., Maier, N.M., Lindner, W., 2004. Investigation on the chromatographic behaviour of hybrid reversed-phase material containing electron donor–acceptor systems II. Contribution of π–π aromatic interaction. Journal of Chromatography A 1054, 43–58.

Jasper, J.P., Hayes, J.M., 1990. A carbon isotope record of CO_2 levels during the late Quaternary. Nature 347, 462–464.

de Leeuw, J.W., van der Meer, F.W., Rijpstra, W.I.C., 1980. On the occurrence and structural identification of long-chain unsaturated ketones and hydrocarbons in sediments. In: Douglas, A.G., Maxwell, J.R. (Eds.), Advances in Organic Geochemistry 1979. Pergamon, Oxford, pp. 211–217.

Malone, T.C., 1992. Effects of water column processes on dissolved oxygen, nutrients, phytoplankton and zooplankton. In: Smith, D.E., Leffler, M., Mackiernan, G. (Eds.), Oxygen Dynamics in Chesapeake Bay. Maryland Sea Grant College, College Park, MD.

Marchand, D.H., Croes, K., Dolan, J.W., Snyder, L.R., 2005. Column selectivity in reversed-phase liquid chromatography. VII. Cyanopropyl columns. Journal of Chromatography A 62, 57–64.

Marlowe, I.T., Brassell, S.C., Eglinton, G., Green, J.C., 1984. Long chain unsaturated ketones and esters in living algae and marine sediments. Organic Geochemistry 6, 135–141.

Marshall, H.G., 1980. Seasonal phytoplankton composition in the Lower Chesapeake Bay and old plantation creek, Cape Charles, Virginia. Estuaries 3, 207–216.

Matucha, M., Jockisch, W., Verner, P., Anders, G., 1991. Isotope effect in gas-liquid chromatography of labelled compounds. Journal of Chromatography A 588, 251–258.

Mercer, J.L., Zhao, M., Colman, S.M., 2005. Seasonal variations of alkenes and U^k_{37} in the Chesapeake Bay water column. Estuarine Coastal and Shelf Science 63, 675–682.

Müller, P.J., Kirst, G., Ruhland, G., von Storch, I., Rosell-Melé, A., 1998. Calibration of alkenone paleotemperature index U^k_{37} based on core tops from the eastern South Atlantic and the global ocean (60N–60S). Geochimica et Cosmochimica Acta 62, 1757–1772.

Officer, C.B., Biggs, R.B., Taft, J.L., Cronin, L.E., Tyler, M.A., Boynton, W.R., 1984. Chesapeake Bay anoxia: origin, development and significance. Science 223, 22–27.

Pagani, M., Arthur, M.A., Freeman, K.H., 1999. Miocene evolution of atmospheric carbon dioxide. Paleoceanography 14, 273–292.

Pahnke, K., Sachs, J.P., Keigwin, L.D., Timmermann, A., Xie, S.-P., 2007. Eastern tropical Pacific hydrologic changes during the past 27000 years from D/H ratios in alkenones. Paleoceanography 22, PA4214.

Prahl, F.G., Wakeham, S.G., 1987. Calibration of unsaturation pattern in long-chain ketone compositions for paleotemperature assessment. Nature 330, 367–369.

Prahl, F.G., Muehlhausen, L.A., Zahnle, D.L., 1988. Further evaluation of long-chain alkenones as indicators of paleoceanographic conditions. Geochimica et Cosmochimica Acta 52, 2303–2310.

Rechka, J.A., Maxwell, J.R., 1988. Unusual long chain ketones of algal origin. Tetrahedron Letters 29, 2599–2600.

Rontani, J-F., Prahl, F.G., Volkman, J.K., 2006. Re-examination of the double bond positions in alkenones and derivatives: biosynthetic implication. Journal of Phycology 42, 800–813.

Sachs, J.P., Schneider, R.R., Eglinton, T.I., Freeman, K.H., Ganssen, G., McManus, J.F., Oppo, D.W., 2000. Alkenones as paleoceanographic proxies. Geochemistry, Geophysics, Geosystems 1. 2000GC000059.

Sachse, D., Sachs, J.P., 2008. Inverse relationship between D/H fractionation in cyanobacterial lipids and salinity in Christmas Island saline ponds. Geochimica et Cosmochimica Acta 72, 793–806.

Schouten, S., Ossebaar, J., Schreiber, K., Kienhuis, M.V.M., Langer, G., Benthien, A., Bijma, J., 2006. The effect of temperature, salinity and growth rate on the stable hydrogen isotopic composition of long chain alkenones produced by *Emiliania Huxleyi* and *Gephyrocapsca Oceanica*. Biogeosciences 3, 113–119.

Smittenberg, R.H., Sachs, J.P., 2007. Purification of dinosterol for hydrogen isotopic analysis using high-performance liquid chromatography-mass spectrometry. Journal of Chromatography A 1169, 70–76.

Taft, J.L., Taylor, W.R., Hartwig, E.O., Loftus, R., 1980. Seasonal oxygen depletion in Chesapeake Bay. Estuaries 3, 242–247.

Turowski, M., Yamakawa, N., Meller, J., Kimata, K., Ikeami, T., Hosoya, K., Tanaka, N., Thotnton, E.R., 2003. Deuterium isotope effects on hydrophobic interactions: the importance of dispersion interactions in the hydrophobic phase. Journal of the American Chemical Society 125, 13836–13849.

Van der Meer, M.T.J., Bass, M., Rijpstra, I.C., Marino, G., Rohling, E.J., Sinninghe Damsté, J.S., Schouten, S., 2007. Hydrogen isotopic compositions of long-chain alkenones record freshwater flooding of the Eastern Mediterranean at the onset of sapropel deposition. Earth and Planetary Science Letters 262, 594–600.

Volkman, J.K., Eglinton, G., Corner, E.D.S., Forsberg, T.E.V., 1980a. Long-chain alkenes and alkenones in the marine coccolithophorid *Emiliania huxleyi*. Phytochemistry 19, 2619–2622.

Volkman, J.K., Eglinton, G., Corner, E.D.S., Sargent, J.R., 1980b. Novel unsaturated straight-chain C_{37}–C_{39} methyl and ethyl ketones in marine sediments and a coccolithophore *Emiliania huxleyi*. In: Douglas, A.G., Maxwell, J.R. (Eds.), Advances in Organic Geochemistry 1979. Pergamon, Oxford, pp. 219–227.

Zhang, Z., Sachs, J.P., 2007. Hydrogen isotope fractionation in freshwater algae. 1: Variations among lipids and species. Organic Geochemistry 38, 582–608.